Gulf of Mexico Gas Hydrate Joint Industry Project Leg II:
Walker Ridge 313 LWD Operations and Results

Ann Cook[1], Gilles Guerin[1], Stefan Mrozewski[1], Timothy Collett[2], & Ray Boswell[3]

Introduction

Two holes, Walker Ridge 313-G (WR 313-G) and Walker Ridge 313-H (WR 313-H), were drilled 0.5 miles apart in the Gulf of Mexico Walker Ridge Block 313 (WR 313). The drilling at WR 313 tests geologic/geophysical predictions of the occurrence of gas hydrate at high concentrations in sand units near the base of gas hydrate stability (Hutchinson *et al*., 2009). McConnell *et al*. (2009) provides a complete assessment of the Walker Ridge site.

Operations

Logging-while-drilling (LWD) operations at the JIP Leg II Walker Ridge Site were conducted using a state of the art bottom hole assembly (BHA), using the Schlumberger MP3, geoVISION, EcoScope, sonicVISION and PeriScope tools. For further description of the BHA, each tool and the tool measurements, see Mrozewski *et al*. (2009).

Hole WR 313-G

After tagging the seafloor (touching the seafloor with the drill bit) at a driller's depth of 6614 ft below the rig floor (fbrf), Hole WR 313-G was spudded at 17h15 on April 18, 2009. Following a spud protocol designed to maintain the condition of the top of the hole (Collett *et al*., 2009), the first 170 ft were drilled while circulating 48 gallons per minute (gpm) of seawater. The flow rate was increased to 385 gpm but fluctuated over the next 200 ft, including a 65 ft-long section where it dropped low enough to adversely impact MWD turbine power. The drill bit rotation was limited to ~15 rotations per minute (rpm) when the bit penetrated seafloor, the bit rate of rotation was increased to ~45 rpm by the time the geoVISION tool entered the hole, and increased to 90 rpm at bit depth of ~180 ft below the seafloor (fbsf). The rate of penetration (ROP) ranged from 350 to over 1000 ft/hr until 240 fbsf when it was stabilized to the target rate of 160 ft/hr (Figure F1).

At some point between pump testing the BHA in shallow water and making the first connection while drilling, the TeleScope tool suffered a failure of one of its three accelerometers that are needed along with three magnetometers to acquire directional surveys. Directional well surveys are required at least every 1000 ft in the Gulf of Mexico, and thus, it was necessary to circulate and work the pipe at that depth for over an hour until permission to proceed was granted by the Minerals Management Service to continue drilling. Adequate surveys were later calculated on shore from data obtained from the remaining operational accelerometers and magnetometers.

Drilling continued relatively smoothly, pumping between 380 and 410 gpm of seawater with intermittent sweeps of 10.5 ppg drilling fluid and suffering occasional pipe stalls, until roughly 1140 fbsf when ROP was reduced temporarily to ~ 100 ft/hr in order to capture higher-resolution images over a zone of interest from 1140 to 1350 fbsf. At 1650 fbsf, it became necessary to backream each stand and drilling became very difficult despite the increase in drilling fluid sweeps. Rotary speed was increased to 120 rpm in response to torque, and the drill string would occasionally pack off despite multiple backreams per stand. A major packoff at 2630 fbsf (stalling the rotary and requiring 140,000 lbs of overpull) prompted a switch to continuously drill with 10 pound per gallon (ppg) water-based drilling fluid. After weighting up the drilling fluid further to 10.5 ppg at 2985 fbsf, the rest of the hole was drilled incident-free. The total depth of 3584 fbsf was reached at 18h45 on April 20 and the hole was displaced with 12 ppg drilling fluid. The LWD tools were brought back to the surface at 08h00 on April 21 and rig down was completed by 10h30 while preparing for transit to Green Canyon block 955.

[1]Borehole Research Group
Lamont-Doherty Earth Observatory
of Columbia University
Palisades, NY 10964
E-mail:
Cook: acook@ldeo.columbia.edu
Guerin: guerin@ldeo.columbia.edu
Mrozewski: stefan@ldeo.columbia.edu

[2]US Geological Survey
Denver Federal Center, MS-939
Box 25046
Denver, CO 80225
E-mail:
tcollett@usgs.gov

[3]National Energy Technology Laboratory
U.S. Department of Energy
P.O. Box 880
Morgantown, WV 26507
E-mail:
ray.boswell@netl.doe.gov

Hole WR 313-H

After completing operations in Green Canyon Block 955 and transiting back to Walker Ridge Block 313, operations resumed with the rigup of the BHA at 12h00 on April 29, 2009. The seafloor was tagged at a driller's depth of 6501 fbrf and Hole WR 313-H was spudded at 19h43. Following a spud protocol designed to maintain good conditions at the top of the hole, the first 60 fbsf were drilled while circulating 200 gpm of seawater and a rate of bit rotation of 14 rpm. Between 60 and 170 fbsf, the pump flow rate was increased to 250 gpm and the bit rotation was increased to 50 rpm, after which point they were increased to 350 gpm and 87 rpm, respectively. At 340 fbsf, the pump rate was again increased to 385 gpm to facilitate MWD directional surveys. For the main section of the hole below ~170 fbsf, the rate of penetration was targeted at 350 ft/hr (Figure F2).

Drilling continued relatively smoothly with drilling fluid sweeps every few stands. The drill bit rotary speed was gradually increased to 133 rpm in response to drilling conditions. At 2000 fbsf, ROP was reduced to 160 ft/hr for a target zone of interest. At the same time, drilling fluid was changed to 10.5 ppg water-based drilling fluid. The well reached a total depth of 3385 fbsf at 20h45 on April 30. The hole was displaced with 10.5 ppg drilling fluid, followed by a 320-barrel "pill" of 12.0 ppg drilling fluid before the BHA was slowly pulled out of hole to surface. The radioactive source was unloaded at 10h15 on May 1 and the tools were laid down shortly after.

Data Quality

Hole WR 313-G

Figure F1 displays selected parameters that illustrate the drilling process in Hole WR 313-G and its possible influence on data quality.

The increases in residual pressure (annulus pressure after subtraction of the hydrostatic pressure) and equivalent circulating density (ECD, a similar measure) at 1650 fbsf and at 2650 fbsf are the result of increases in the drilling fluid density that were necessary to support the drilling. No changes in pressure were observed that suggested the release of free gas or other hazards.

The ROP curve, averaged over 5 ft intervals, indicates cyclical spikes that are artifacts due to speed, depth, and/or depth tracking fluctuations occurring immediately before, during and after pipe connections. As mentioned in the Operations section, ROP is lowered to 100 ft/hr in the intervals of interest. Most logs are not significantly affected by the high ROP used during JIP Leg II. The EcoScope geochemical logs, however, were not able to be properly calibrated due to the high ROP, and thus none of the geochemical logs report reliable measurements.

Ultrasonic and density calipers reveal the typically enlarged near-seafloor borehole. Below 582 fbsf, the hole is in very good condition and rarely exceeds 8.75 inches in diameter. Notable washouts, where density and porosity data are unreliable, occur at 614, 896, 1645, 2441 and 2894 fbsf. No caliper is available for the 6.75 inch hole before it is enlarged to 8.50 inches (Mrozewski *et al*., 2009).

EcoScope data, which includes density measurements, are only acquired after the drilling fluid pump flow rate is sufficient to power the tool, which in Hole WR 313-G occurred at 95 fbsf. When the Ecoscope tool is on the geoVISION's gamma ray reads appreciably higher than the EcoScope gamma ray because, unlike the EcoScope, the geoVISION is not compensated for minitron-induced oxygen activation (Figure F3).

Between 218 and 281 fbsf, and again a few feet deeper, the EcoScope's power-intensive minitron turned off when the drilling fluid flow dropped, although the MWD tool and the rest of the EcoScope sensors remained functional. When the minitron is off, the geoVISION's gamma ray matches that of the EcoScope (Figure F3).

The difficult drilling conditions, most notably the inability to effectively remove cuttings and reduce borehole cavings due to insufficient drilling fluid weight (Collett *et al*., 2009) had an adverse effect on the geoVISION images. When repeatedly lifting off-bottom and alternately stretching and compressing the drillstring and BHA during stalls and packoffs, the LWD depth tracking becomes impaired; this causes distinctive horizontal lines, smears, and/or truncated features in the images.

At a depth of roughly 2500 fbsf, the MP3 tool failed, resulting in the complete loss of both real-time and recorded MP3 data below 2465 fbsf.

The depths relative to seafloor were fixed for all of the LWD logs by identifying the step change in the geoVISION

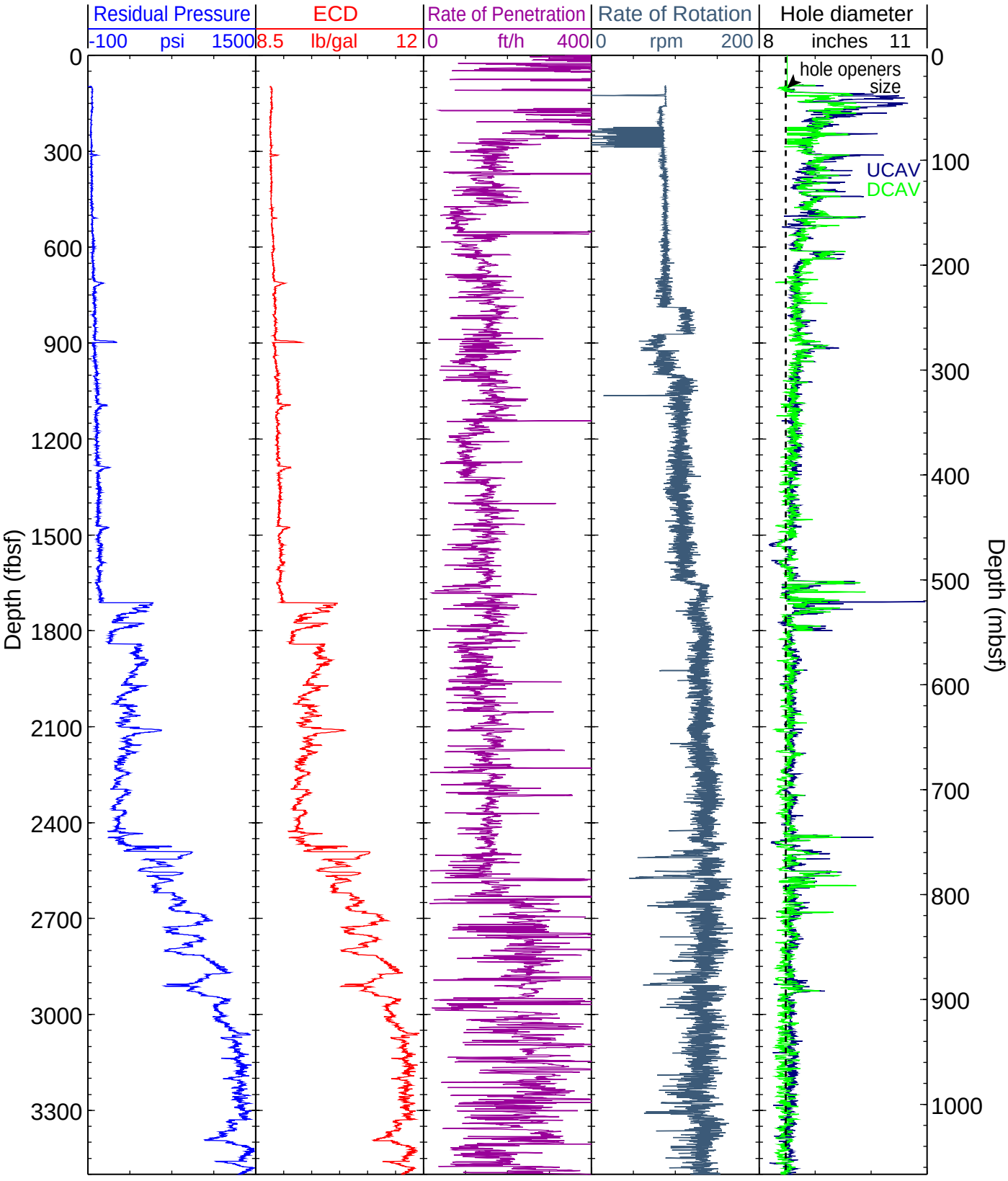

Figure F1: *Monitoring and quality control LWD/MWD logs from Hole WR 313-G. Residual Pressure = Pressure in the annulus after subtraction of the hydrostatic pressure; ECD = Equivalent Circulating Density = effective density of the fluid exerting pressure against the borehole formation; UCAV = Ultrasonic caliper, DCAV = Density caliper.*

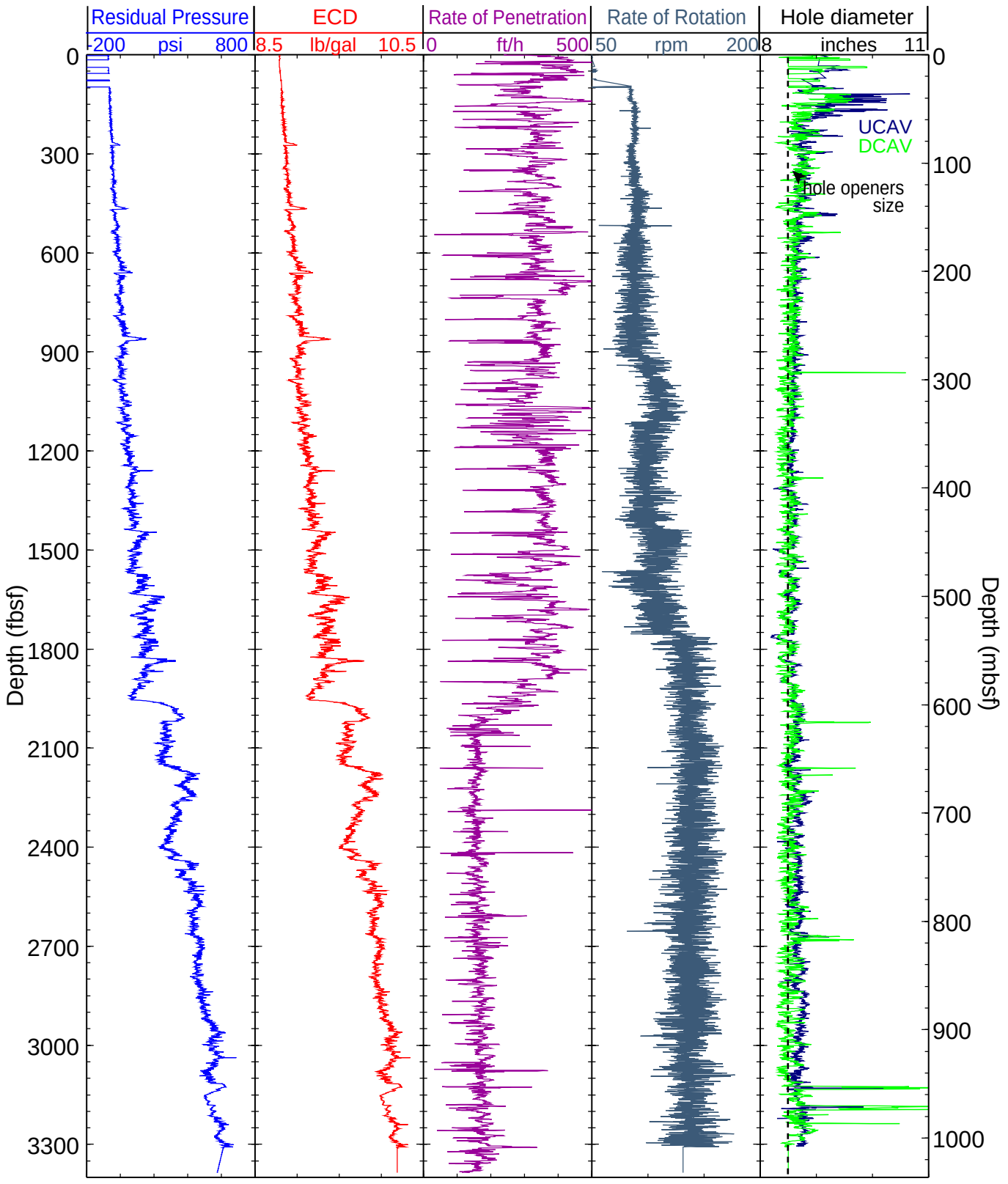

Figure F2: *Monitoring and quality control LWD/MWD logs from Hole WR 313-H. Residual Pressure = Pressure in the annulus after subtraction of the hydrostatic pressure; ECD = Equivalent Circulating Density = effective density of the fluid exerting pressure against the borehole formation; UCAV = Ultrasonic caliper, DCAV = Density caliper.*

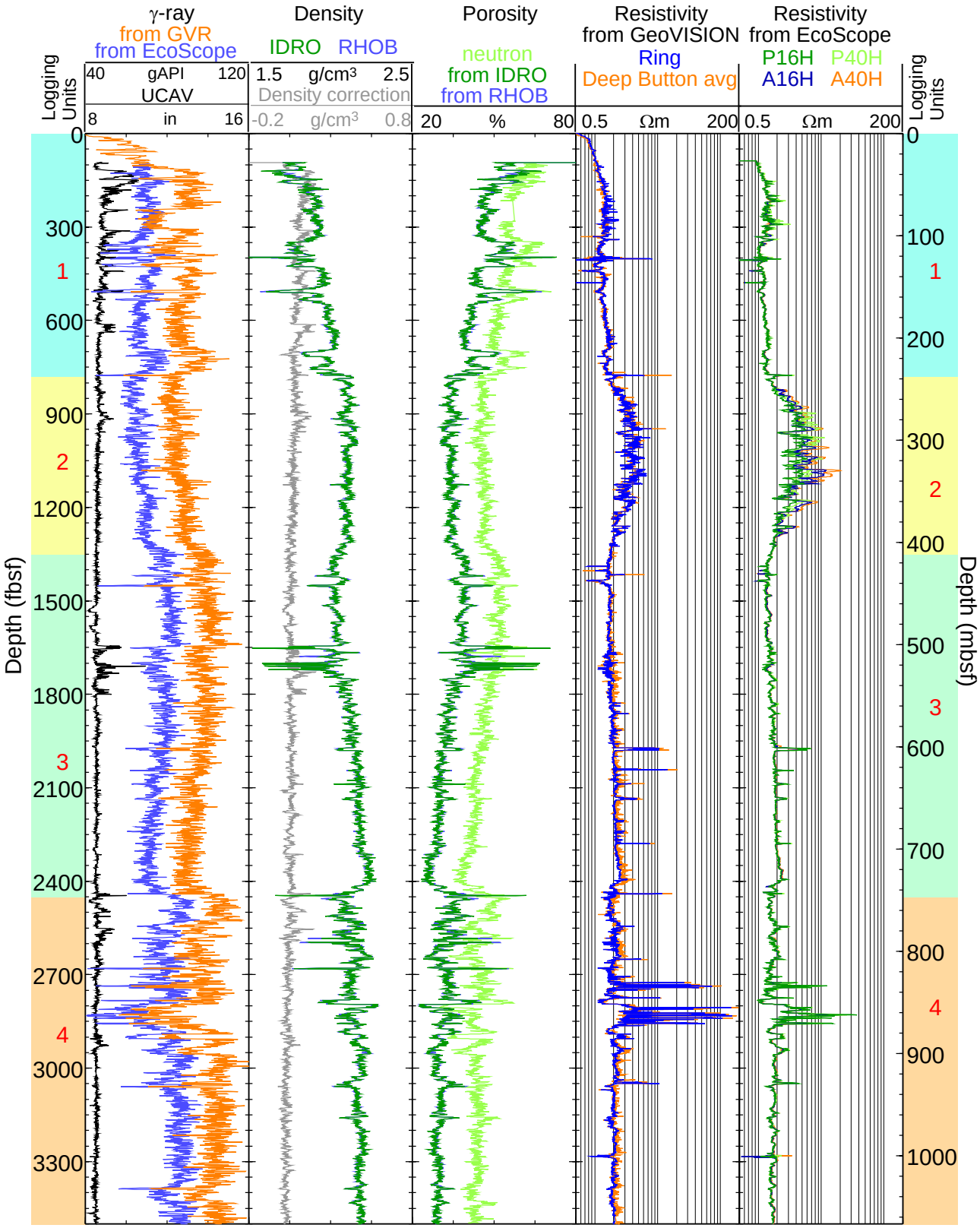

Figure F3: *Summary of LWD log data from Hole WR 313-G. gAPI = American Petroleum Institute gamma ray units, RHOB = Bulk density (EcoScope), IDRO = Image-derived density (EcoScope); neutron = "Best thermal neutron porosity"; (EcoScope); Ring = Ring resistivity (geoVISION); PXXH = Phase-shift resistivity at 2 MHZ and a transmitter-receiver spacing of XX inches. (EcoScope); AXXH = Attenuation resistivity measured at 2 MHz and a transmitter-receiver spacing of XX inches. (EcoScope). Logging Units as described in this report are shown.*

gamma ray log at the seafloor. For Hole WR 313-G, the gamma ray log identified the seafloor at 6616 fbrf, 2 ft below the depth estimated initially by the drillers. The rig floor logging datum was located 52 ft above sea level.

Hole WR 313-H

Figure F2 displays selected parameters that illustrate the drilling process for Hole WR 313-H and its possible influence on data quality. The only changes observed in borehole pressure were due to increases in drilling fluid density; changes in drilling fluid density were made to support drilling. No change in borehole pressure was observed that suggested the release of free gas or other hazards.

The downhole log for ROP, averaged over 5 ft depth intervals, indicates cyclical spikes that are artifacts due to speed, depth, and/or depth tracking fluctuations occurring immediately before, during and after pipe connections. The ROP spikes occasionally correspond with horizontal lines in the geoVISION resistivity images that are offset up the hole by the 61 ft sensor depth offset. The images are also marred by dark, incongruous pixelation in high-resistivity zones; these are manifestations of null values in the raw data, a result of a problem in the current geoVISION software (Figure F4).

Most logs are not significantly affected by the high ROP used during JIP Leg II. The EcoScope geochemical logs, however, were not able to be properly calibrated due to the high ROP, and thus none of the geochemical logs report reliable measurements.

Ultrasonic and density calipers, as well as the resistivity images, reveal typical near-seafloor borehole enlargement. Below 348 fbsf, the hole is in very good condition and its diameter rarely exceeds 8.75 inches. Notable washouts, where density and porosity data are unreliable, occur at 2258, 2666, 3123 and 3181 fbsf.

EcoScope data are only acquired once flow past the MWD turbine is sufficient to power the tool, which in Hole WR 313-H occurred at 94 fbsf for density measurements. When the EcoScope tool is on, the geoVISION's gamma ray reads appreciably higher than the EcoScope's because the geoVISION is not compensated for minitron-induced oxygen activation (Figure F5).

The depths relative to seafloor were fixed for all of the LWD logs by identifying the step change in the geoVISION gamma ray log at the seafloor. For Hole WR 313-H, the gamma ray log identified the seafloor at 6501 fbrf, in agreement with the initial depth estimated by the drillers. The rig floor logging datum was located 51 ft above sea level.

Interpretation of LWD Logs

Logging Displays Overview

The combined analysis of the different logs and images recorded by the LWD tools delineates several logging units with distinct trends that can be observed in the two wells drilled in Walker Ridge Block 313. Most of these trends can be tied to the seismic stratigraphy described in detail in the Walker Ridge 313 Site Summary (McConnell *et al.*, 2009).

Figures F3 and F5 show the main logs recorded by the geoVISION and the EcoScope tools in Holes WR 313-G and WR 313-H. As noted in the ***Data Quality*** section, the offset between the gamma ray logs recorded by the two tools is the result of the influence of the minitron-activated gamma rays on the readings of the geoVISION. Despite this offset, the two tools display identical trends, and the EcoScope gamma ray is used in the following discussion.

Figures F6 and F7 give a summary of some of the images recorded by the geoVISION and the EcoScope tools. The same measurements are made for the images and the associated one-ensional log curves. For example, the deep resistivity log is the average of the deep button resistivity image. The azimuthal images illustrate the influence of structure and heterogeneity on the measurements captured by the one-dimensional logs.

Figures F8 and F9 display the compressional velocity data recorded by the MP3 and the sonicVISION tools. In addition to the V_p logs, the display of the monopole waveforms and of the slowness-time coherence (STC) projections used to derive V_p provides an assessment of the quality of the acoustic data and of the attenuating effect of gas hydrate. In general, there is excellent correlation between the MP3 and sonicVISION compressional velocity in both Holes WR 313-G and WR 313-H.

Logging Units

Resistivity and compressional velocity logs provide a guide to the variations in lithology and gas hydrate occurrence. The gamma ray and density logs are primarily used to determine lihology and the logging units.

Logging Unit 1 extends from the surface to 780 fbsf in Hole WR 313-G and to 540 fbsf in Hole WR 313-H. It is characterized by a steady increase with depth in resistivity and sonic velocity, with relatively uniform gamma ray readings and an overall increase in density interrupted by three 80- to 100-ft thick intervals with apparently lower density, possibly the results of bad hole conditions. The similar characteristics of these intervals, channel deposits with thin low gamma ray sands, show a strong lateral continuity between the two holes. The tops of these intervals (~350 fbsf in WR 313-G and ~200 fbsf in WR 313-H) could coincide with Seismic Horizon A (McConnell *et al*., 2009).

With a top defined by a drop in gamma ray and increase in density (780 fbsf in WR 313-G, 540 fbsf in WR 313-H), Logging Unit 2 is characterized by an almost uniform density and by gamma ray values lower than in Logging Unit 1. Most significantly, this unit is defined by higher velocity and resistivity values, most apparent in the bright electrical images in Figures F6 and F7, that suggest the occurrence of gas hydrate throughout most of this unit. A close inspection of the resistivity images in this logging unit suggests that most of the gas hydrate occurs in thin sand layers and near-vertical fractures.

The top of Logging Unit 3 (1300 fbsf in WR 313-G and 1050 fbsf in WR 313-H) appears to coincide with Seismic Horizon B (McConnell *et al.*, 2009) and is marked by a sharp drop in velocity, resistivity and density, as well as an increase in gamma ray, which is indicative of more clay-rich sediments. Gamma ray values decrease subtly but steadily down the unit, while density, resistivity all increase with depth, suggesting an overall fining upward formation. Across the entire unit in both wells, thin layers (a few feet thick) with low gamma ray values, high resistivity and velocity and low waveform amplitudes are likely hydrate-bearing sands.

The boundary between Logging Units 3 and 4 is defined by a sharp gamma ray increase and a velocity drop (at 2450 fbsf in WR 313-G and 2000 fbsf in Hole WR 313-H) that are likely associated with the unconformity defining Seismic Horizon C (McConnell *et al.*, 2009). While all the logs show some degree of variability between the two wells within this unit - in particular the gamma ray and resistivity logs - the trends are generally uniform except for a noticeable ~100 foot-thick sand sequence between ~2800 and 2900 fbsf in Hole WR 313-G suggesting a high concentration of gas hydrate in a thick sand unit identified as the “blue” reflector on seismic. This interval also crosses Hole WR 313-H at ~2300 fbsf, but the sands are much thinner, have higher clay-content, and lower porosity, and display lower resistivity. Thus, there is lower gas hydrate content in this interval. Below the blue interval, most logs are almost uniform except for two sand units between ~2640 and 2700 fbsf in Hole WR 313-H, with very low gamma ray values and very high resistivity and velocity values indicative of high gas hydrate concentrations. These sands coincide with Seismic Horizon D (the “orange” reflector). Correlative, but less well developed sand units were also recognized in Hole WR 313-G between 3350 and 3450 fbsf, but below the theoretical base of the gas hydrate stability zone and without indication of gas or gas hydrate.

LWD Borehole Images

The geoVISION and EcoScope tools generate high-resolution 360° images of borehole log data. The EcoScope tool produces images of density and hole radius (computed on the basis of the density correction which is a function of borehole standoff) as well as gamma ray and photoelectric factor. The geoVISION produces a gamma ray image and shallow, medium and deep depth of investigation resistivity images.

Figures F6 and F7 show some of the LWD images collected by the EcoScope and geoVISION tools. The unwrapped images are about 70 cm wide (for a 8.5 inch diameter borehole) and the vertical scale is compressed relative to the horizontal by a factor of about 200:1. These high-resolution images can be used for detailed sedimentological and structural interpretations and to image gas hydrate distribution in sediments (e.g., in layers, nodules, fractures). Gas hydrate-bearing sediments exhibit high resistivity within intervals of uniform or low bulk density. By comparison, layers with high resistivities and high densities are likely to be low porosity, compacted, or carbonate-rich sediments.

One prominent feature on the LWD images from Hole WR 313-G is the borehole breakouts which occur at several intervals throughout the hole. Borehole breakouts appear in the unwrapped images as two parallel vertical features which are usually conductive (or dark colored). These features are caused by borehole failure, or spalling, in the direction of minimum horizontal stress. Figure F6 shows the breakouts in the resistivity images in tracks 6 and 7. The breakouts appear intermittently over the majority of

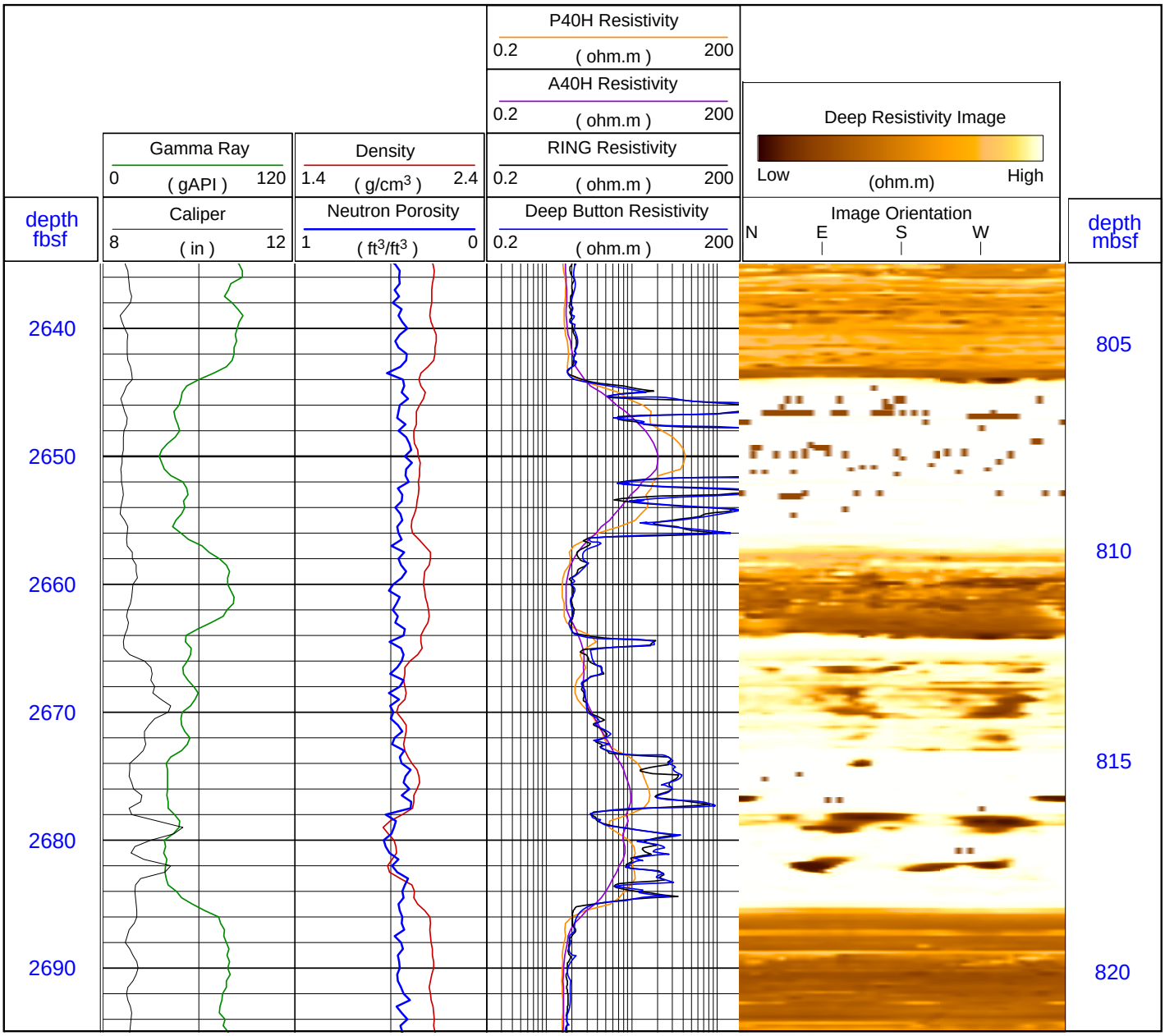

Figure F4: *Logs and LWD resistivity image from 2635-2695 fbsf in well WR 313-H depicting the target sand layer. Ring = Ring resistivity (geoVISION); P40H = Phase-shift resistivity at 2 MHZ and a transmitter-receiver spacing of 40 inches (EcoScope); A40H = Attenuation resistivity measured at 2 MHz and a transmitter-receiver spacing of 40 inches. (EcoScope).*

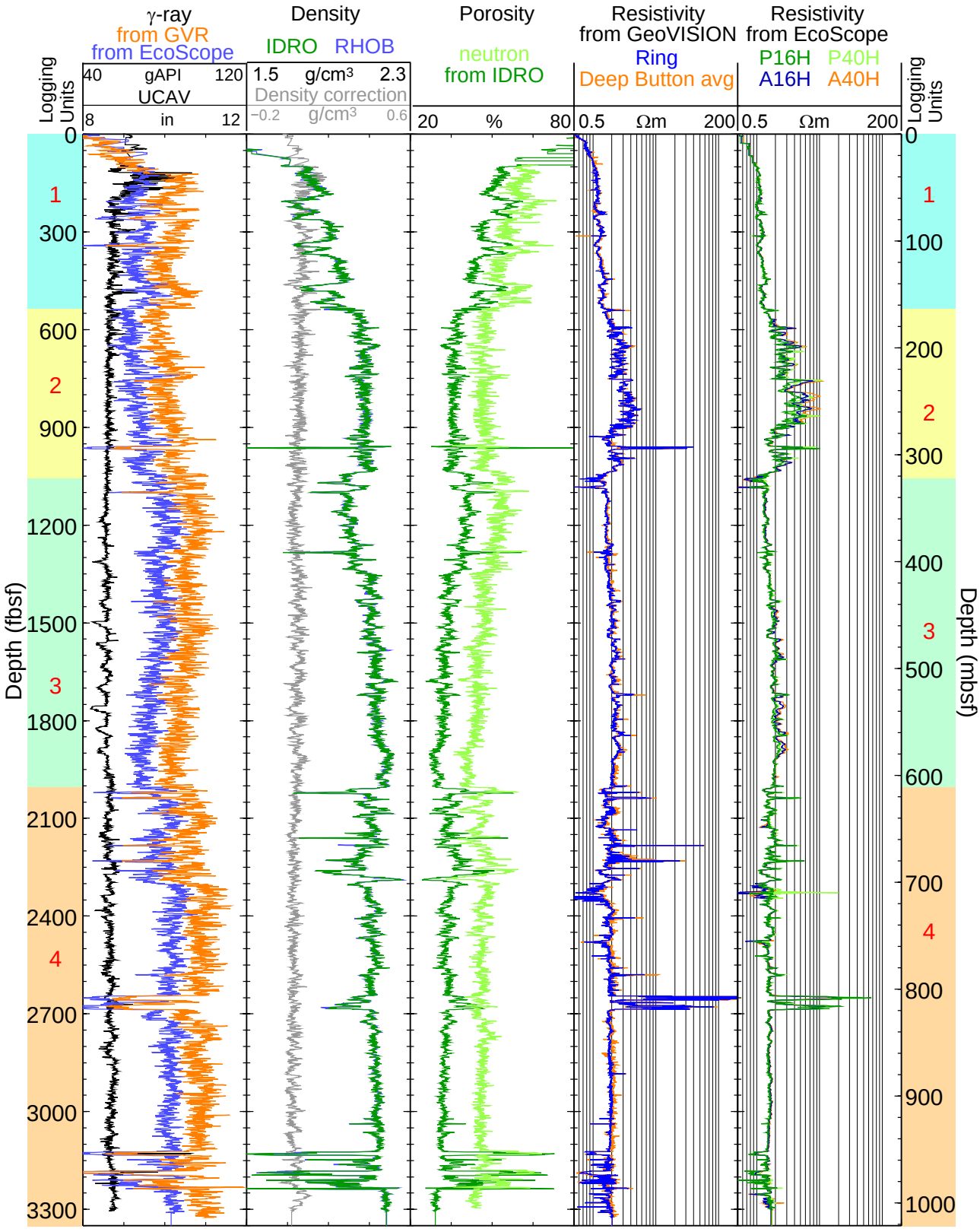

Figure F5: *Summary of LWD log data from Hole WR 313-H. gAPI = American Petroleum Institute gamma ray units, RHOB = Bulk density (EcoScope), IDRO = Image-derived density (EcoScope); neutron = "Best thermal neutron porosity"; (EcoScope); Ring = Ring resistivity (geoVISION); PXXH = Phase-shift resistivity at 2 MHZ and a transmitter-receiver spacing of XX inches. (EcoScope); AXXH = Attenuation resistivity measured at 2 MHz and a transmitter-receiver spacing of XX inches. (EcoScope). Logging Units as described in this report are shown.*

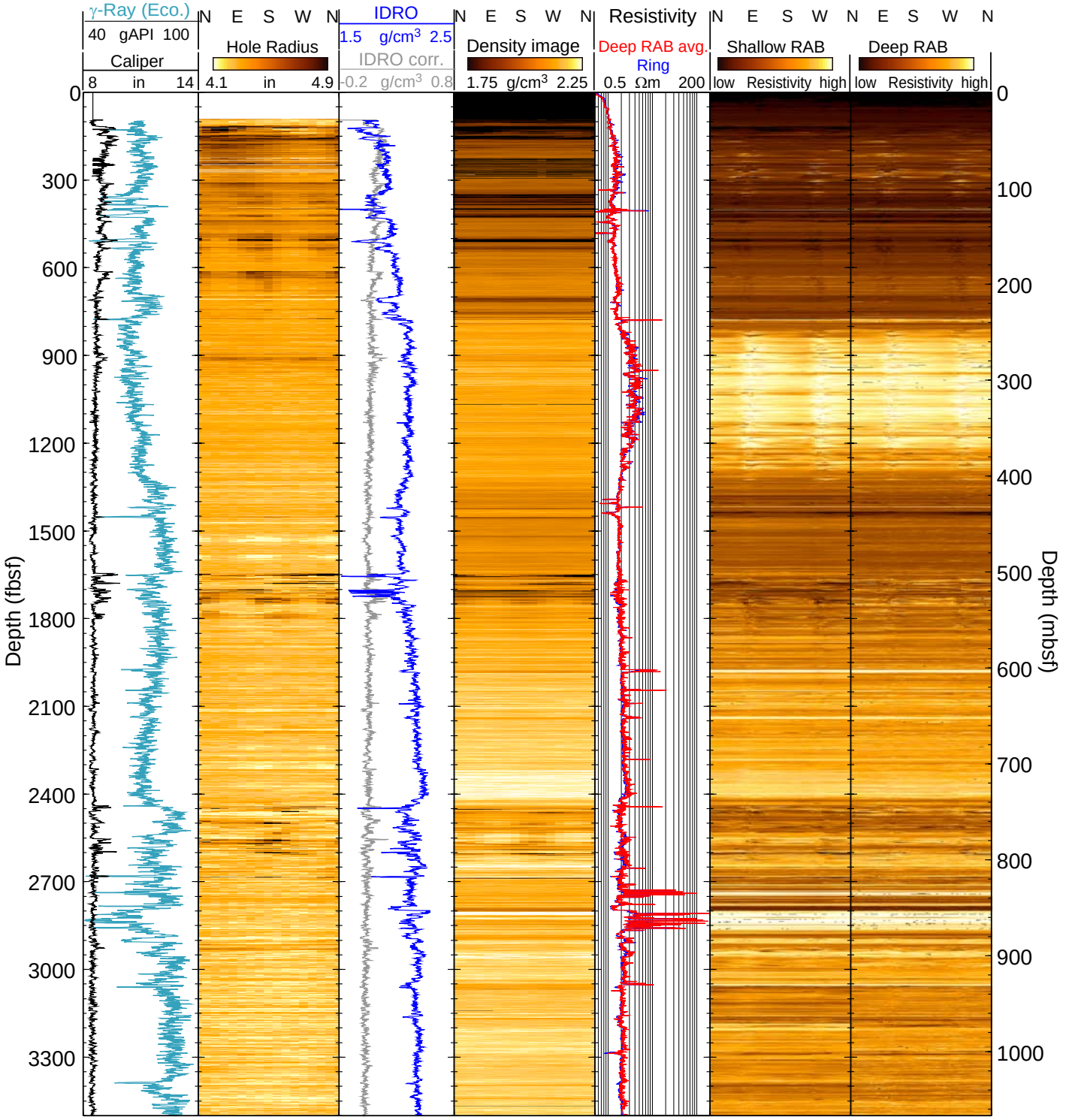

Figure F6: *LWD image data from Hole WR 313-G. gAPI = American Petroleum Institute gamma ray units; RAB = Resistivity-at-the-bit images obtained by the geoVISION tool; IDRO = Image-derived density (EcoScope). The cardinal directions indicate orientation of the images.*

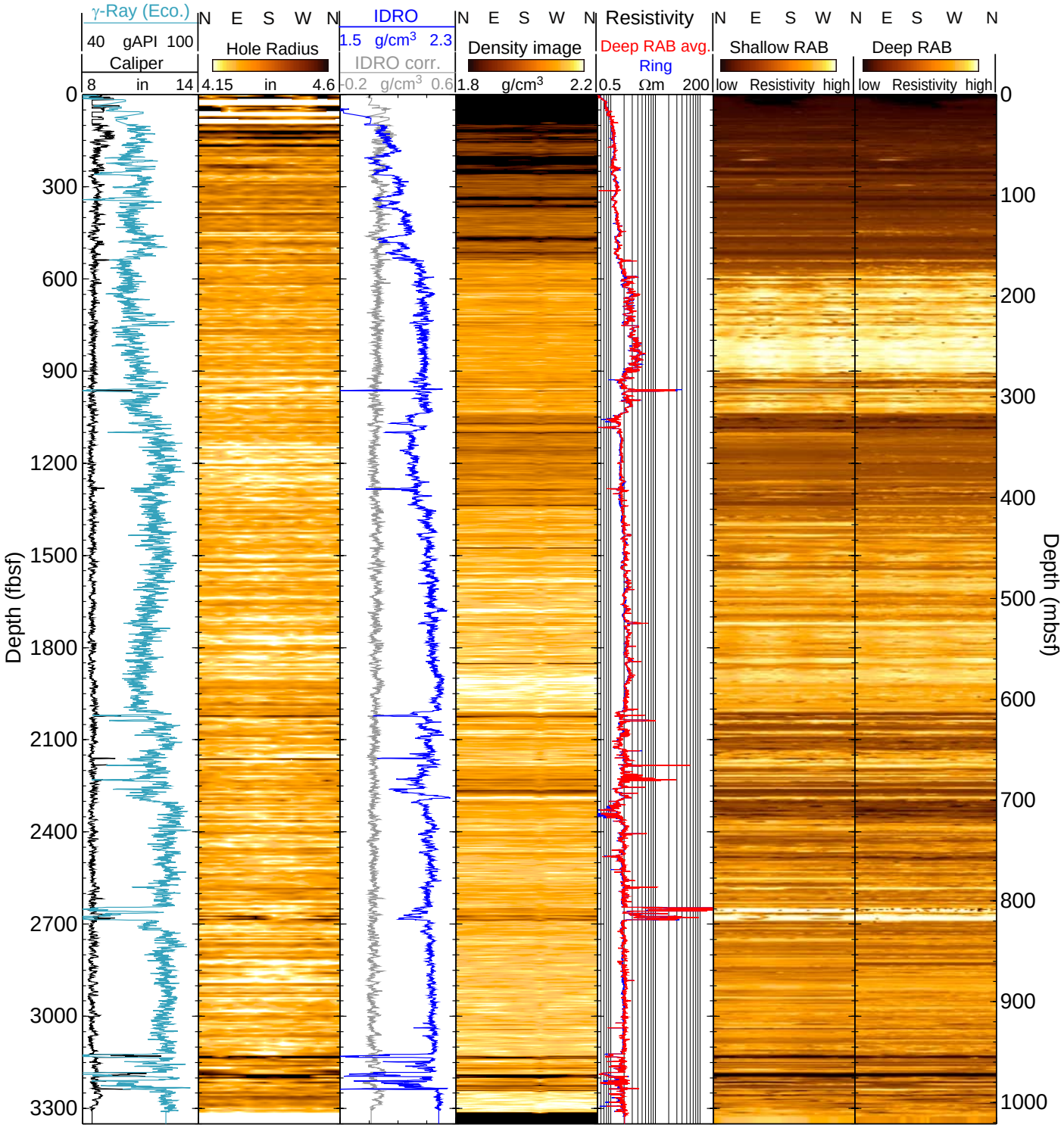

Figure F7: *LWD image data from Hole WR 313-H. gAPI = American Petroleum Institute gamma ray units; RAB = Resistivity-at-the-bit images obtained by the geoVISION tool; IDRO = Image-derived density (EcoScope). Orientation of the images is indicated by the cardinal directions labeled at the top.*

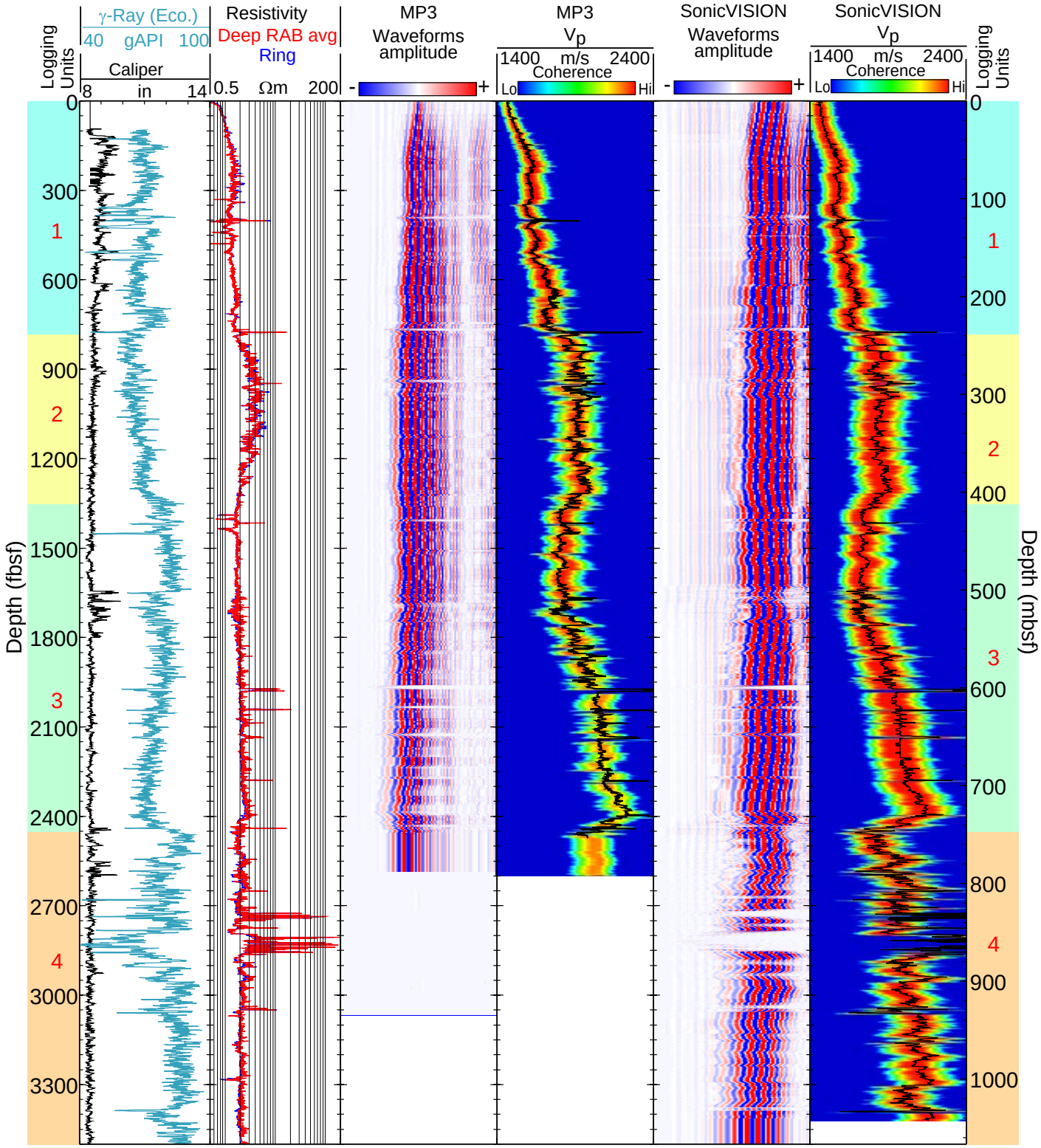

Figure F8: *Sonic waveform data and P-wave velocities recorded by the MP3 and sonicVISION acoustic tools in Hole WR 313-G. Coherence projections resulting from the Slowness-Time Coherence processing give an indication of the quality and reliability of the data. V_p = P-wave velocity. Logging Units as described in this report are shown.*

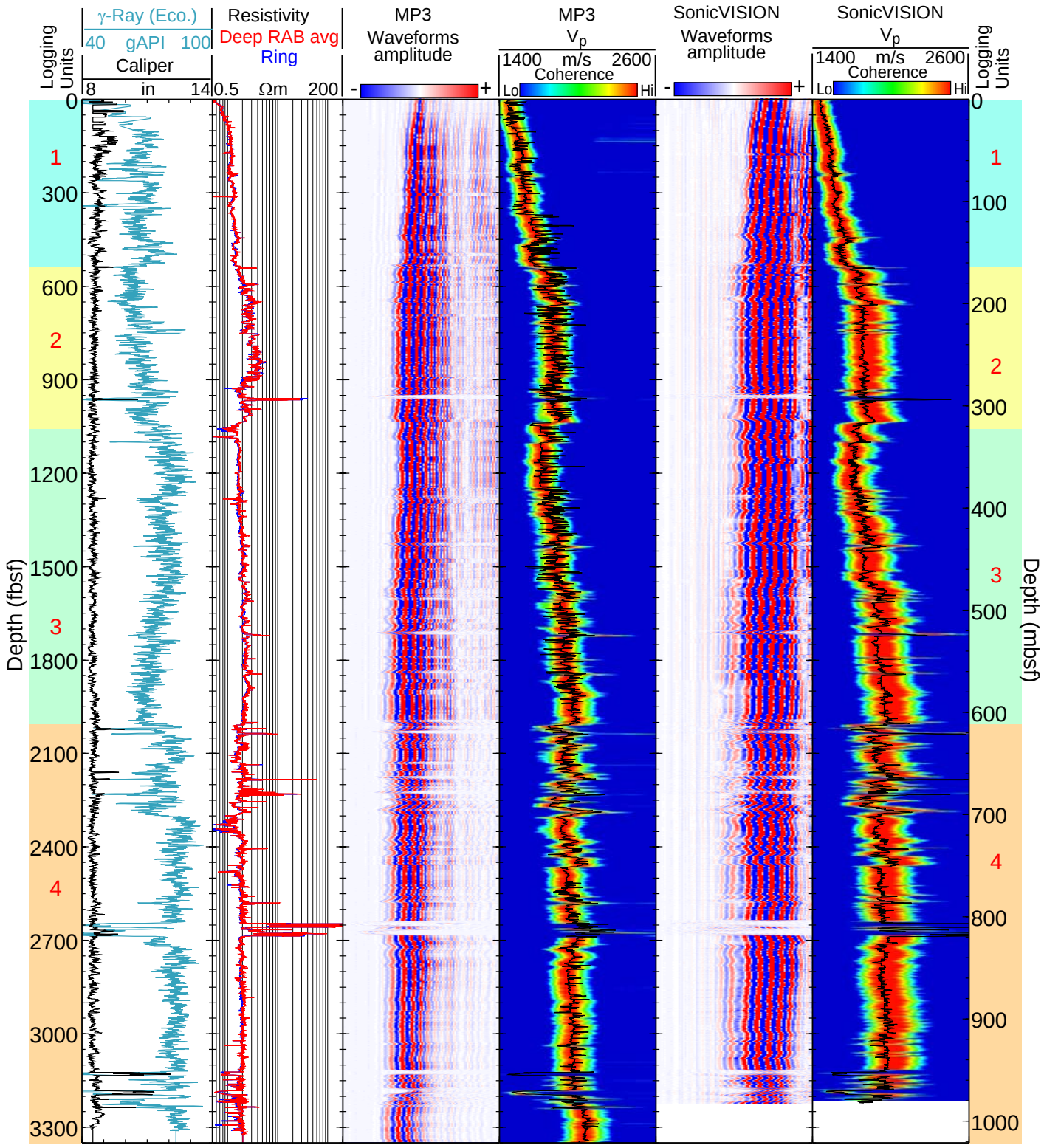

Figure F9: *Sonic waveform data and P-wave velocities recorded by the MP3 and sonicVISION acoustic tools in Hole WR 313-H. Coherence projections resulting from the Slowness-Time Coherence processing give an indication of the quality and reliability of the data. V_p = P-wave velocity. Logging Units as described in this report are shown.*

Hole WR 313-G. The breakouts orient ~E-W, meaning the maximum horizontal stress in the shallow sediments is ~N-S.

The presence of gas hydrate is usually believed to stabilize the borehole, as was observed on Hydrate Ridge during Ocean Drilling Program Leg 204 (Tréhu *et al*., 2003). In Hole WR 313-G, however, the breakouts occur through sections that are hydrate-bearingthrough sections that are both gas hydrate-bearing and gas hydrate free. Breakouts occur prominently in the gas hydrate-filled fracture interval from 750 fbsf to 1300 fbsf and effectively mask other features, including gas hydrate-filled fractures. Interestingly, in the fracture sections the breakouts appear more resistive than the surrounding sediment. In the deeper, thick hydrate-bearing sands from 2725 to 2860 fbsf borehole breakout do not occur, while in the thinner sands, peppered throughout WR 313-G, are usually affected by the breakouts.

Gas Hydrate

In WR 313-G and WR 313-H, numerous gas hydrate-bearing intervals were identified throughout both holes. In WR 313-G, the highest resistivities, which are indicative of hydrate-bearing-sediments, occur in two intervals from 2725 to 2745 fbsf and from 2805 to 2860 fbsf (Figures F10 and F11). The WR 313-G sands are laminated with resistivity peaks near 200 Ω-m adjacent to resistivities of only a few Ω-m. In Hole WR 313-H, the apparent hydrate-bearing sand section is thicker and occurs in two intervals from 2644 to 2656 fbsf and from 2663 to 2685 fbsf (Figure F4). In addition to the more prominent hydrate occurrences, many small gas hydrate-filled sands a few feet thick or less occur throughout both holes.

Also discovered at both Walker Ridge holes were large intervals dominated by near-vertical gas hydrate-filled fractures in fine-grained sediments. Intervals containing high-angle gas hydrate-filled fractures can be identified from the propagation resistivity measurements when the P40H and/or the A40H resistivity curves exceed the P16L and A16L resistivity curves due to the electrical anisotropy caused by the near-vertical fracture planes (Figures F3 and F5). Horizontal fracture or beds do not cause electrical anisotropy because logging tools are designed to detect horizontal layers.

On the borehole resistivity images, gas hydrate-filled fractures appear as resistive sinusoids as shown on Figure F12 in Hole WR 313-H. Near the peaks and troughs of the resistive sinusoids, bright resistive halos can appear due to the current avoiding the path containing gas hydrate. The halos are often adjacent to dark conductive partial sinusoids where the current path is concentrated. In Hole WR 313-G, the near-vertical gas hydrate-filled fractures likely occur between ~815 and 1300 fbsf, as defined by the separation in the propagation resistivity curves. Only a few fractures are visible on the resistivity images in this interval because borehole breakouts dominate the resistivity contrast, causing most of the gas hydrate-filled fractures to be effectively invisible (for example, see Figure F13). In Hole WR 313-H, the near-vertical gas hydrate-filled fractures are clearly visible on the resistivity images from ~590 to 1030 fbsf, which coincides with the separation in the propagation resistivity curves (Figure F12). Some of the fracture sinusoids span up to 10 ft, which suggest dip angles exceeding 80 degrees. Also in Hole WR 313-H some resistive fractures that are likely gas hydrate filled also occur from 1440 to 1900 fbsf. There is no appreciable increase in the one-dimensional measured resistivities or a separation in propagation resistivity curves in that interval that would suggest the interval is gas hydrate-bearing. If the interval is gas hydrate-bearing, it likely has very low gas hydrate saturations on the order of 1%.

The techniques used to determine gas hydrate saturation from the measured resistivity are described in Mrozewski *et al*. (2009). In Hole WR 313-G, a water-saturated sandy-clay interval from 2150 to 2400 fbsf was selected to calibrate the cementation exponent *m* for the target sands, and for that interval, $R_t = R_0 = (R_w / \phi m)$. This sandy clay interval, where gamma ray values are 65-70 API, is not as clean as the laminated target sands that have gamma ray values lower than 50 API. However, this interval is the most similar to the target sand and is used for calibrating *m*; an *m* value of 1.8 is determined to be the best match for the sandy clay interval and was applied to sediments below 1700 fbsf. An *m* value of 2 is determined from the water-saturated clay interval from 1500 to 1600 fbsf, and applied to the sediments above 1700 fbsf to determine gas hydrate saturations for the gas hydrate-filled fracture interval (Figures F14 and F15). In the laminated sands from 2725 to 2744 fbsf in Hole WR 313-G, Archie's equation suggests gas hydrate saturations that peak at 75-90%, however, these high saturations are only 5 ft of the total 19 ft section. The high saturation sediments are adjacent to low saturation sediments with hydrate saturation less than 20%. The

basal sand from 2804 to 2860 fbsf has sand laminations with Archie saturations between 40-80%; the gamma ray in this basal sand interval is cleaner than the upper sand, and saturations in the dirtier laminations contain 15-30% gas hydrate. In the gas hydrate-filled fracture section, Archie's equation suggests gas hydrate saturations near 20-30%, however, current research suggests the gas hydrate saturations calculated using Archie's equation in high-angle gas hydrate-filled fractures significantly overestimates the gas hydrate saturation, and either Archie's equation needs to be modified or a different technique needs to be used (Lee and Collett, 2009).

In Hole WR 313-H, a few water-saturated sand intervals (the "green" horizon: see Hutchinson *et al*., 2009) appear near the bottom of the hole, from 3100 to 3250 fbsf. While the hole is significantly enlarged in these water-saturated intervals, attempts were made to calibrate *m* in these intervals with both neutron porosity and density porosity with RING and A40H resistivity. The results, however, were statistically insignificant and suggested unrealistic *m* values ranging from 3 to 7. Instead, the *m* = 1.8, determined from Hole WR 313-G, was applied to the target sand intervals. For the rest of Hole WR 313-H, *m* = 1.9 was determined for the water-saturated clays from 1400 to 1700 fbsf (Figures F16 and F17).

The top of the hydrate bearing sand interval from WR 313-G (from 2725 to 2744 fbsf and 2805 to 2860 fbsf) are traced on the seismic along the Blue Horizon, and intersect WR 313-H updip at ~2200 fbsf. There are some smaller laminated sands in this interval in WR 313-H, from 2180-2186 mbsf and 2223-2235 fbsf that appear to contain gas hydrate ~60% saturation. These laminated sands are thinner, contain more clay and have lower hydrate saturations in WR 313-H than the sands in WR 313-G from 2725 to 2860 fbsf. These sands in WR 313-H could be a thinned sand unit from WR 313-G or a new sand interval.

In addition to the shallow laminated hydrate bearing sands, WR 313-H also contains deeper, hydrate bearing sand units, which were the drilling target. In the top sand layer from 2644 to 2656 fbsf, Archie's equation suggests saturations between 75-90%. In the basal target sand unit from 2663 to 2685 fbsf, Archie's equation suggests slightly lower saturations of about 40-70%. In the gas hydrate-filled fracture intervals, from 815-1300 fbsf in Hole WR 313-G and in from 590-1030 fbsf in Hole WR 313-H. Archie's equation suggests gas hydrate saturations near 20-30%, in the inferred gas hydrate-filled fracture section however, current research suggests the gas hydrate saturations calculated using Archie's equation in high-angle gas hydrate-filled fractures significantly overestimates the gas hydrate saturation and either Archie's equation needs to be modified (Lee and Collett, 2009) or a different saturation technique applied.

The gas hydrate-filled fracture interval with increased resistivity (from 815-1300 in Hole WR 313-G and from 590 to 1030 in Hole WR 313-H) occur within the common unit on the 3-D seismic (McConnell *et al*., 2009). The fractures may chiefly form in this interval due to slight differences in lithology or pore characteristics.

Conclusions

At Walker Ridge 313, logging revealed gas hydrate in both sand and fine-grained sediments. The sand units were predicted to be hydrate-bearing from pre-drilling seismic assessments, but the near-vertical gas hydrate filled fractures were not predicted (McConnell *et al.*, 2009). The most important discoveries at Walker Ridge 313 include:

- Gas hydrate-bearing sands were observed with saturations over 50% for a total of 25 ft were encountered in Hole WR 313-G.
- Over 30 ft of gas hydrate-bearing sands with saturations over 50% were observed in Hole WR 313-H.
- A laminated gas hydrate-bearing sand near 2800 fbsf Hole WR 313-G, was determined to extend updip to 2200 fbsf in Hole WR 313-H.
- Over 500 ft of near-vertical gas hydrate filled fractures in fine-grained sediments was discovered in both Holes WR 313-G and WR 313-H.

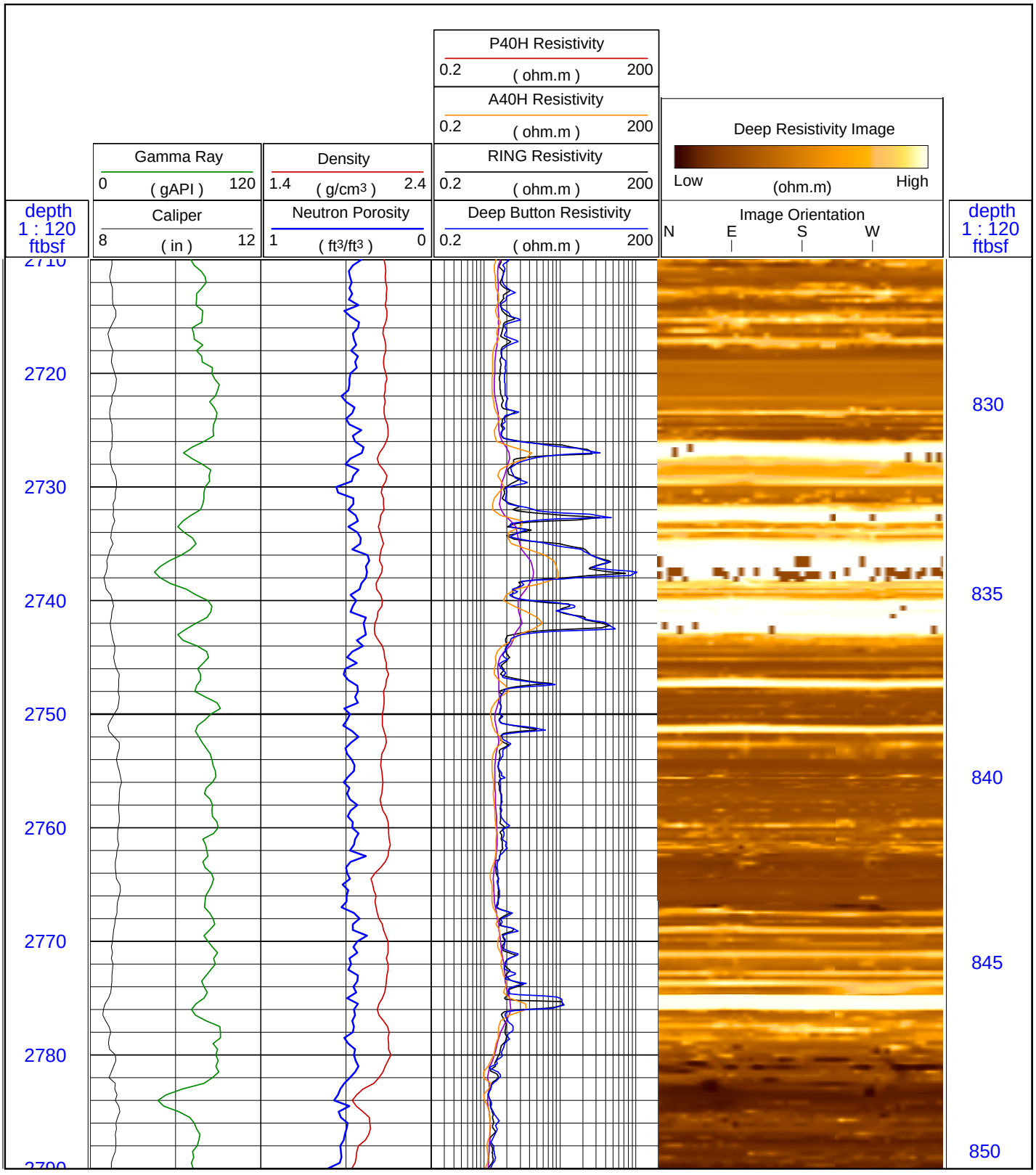

Figure F10: *Logs and LWD resistivity image from 2710-2790 fbsf in Hole WR 313-G depicting the upper target sand layer. Ring = Ring resistivity (geoVISION); P40H = Phase-shift resistivity at 2 MHZ and a transmitter-receiver spacing of 40 inches (EcoScope); A40H = Attenuation resistivity measured at 2 MHz and a transmitter-receiver spacing of 40 inches. (EcoScope).*

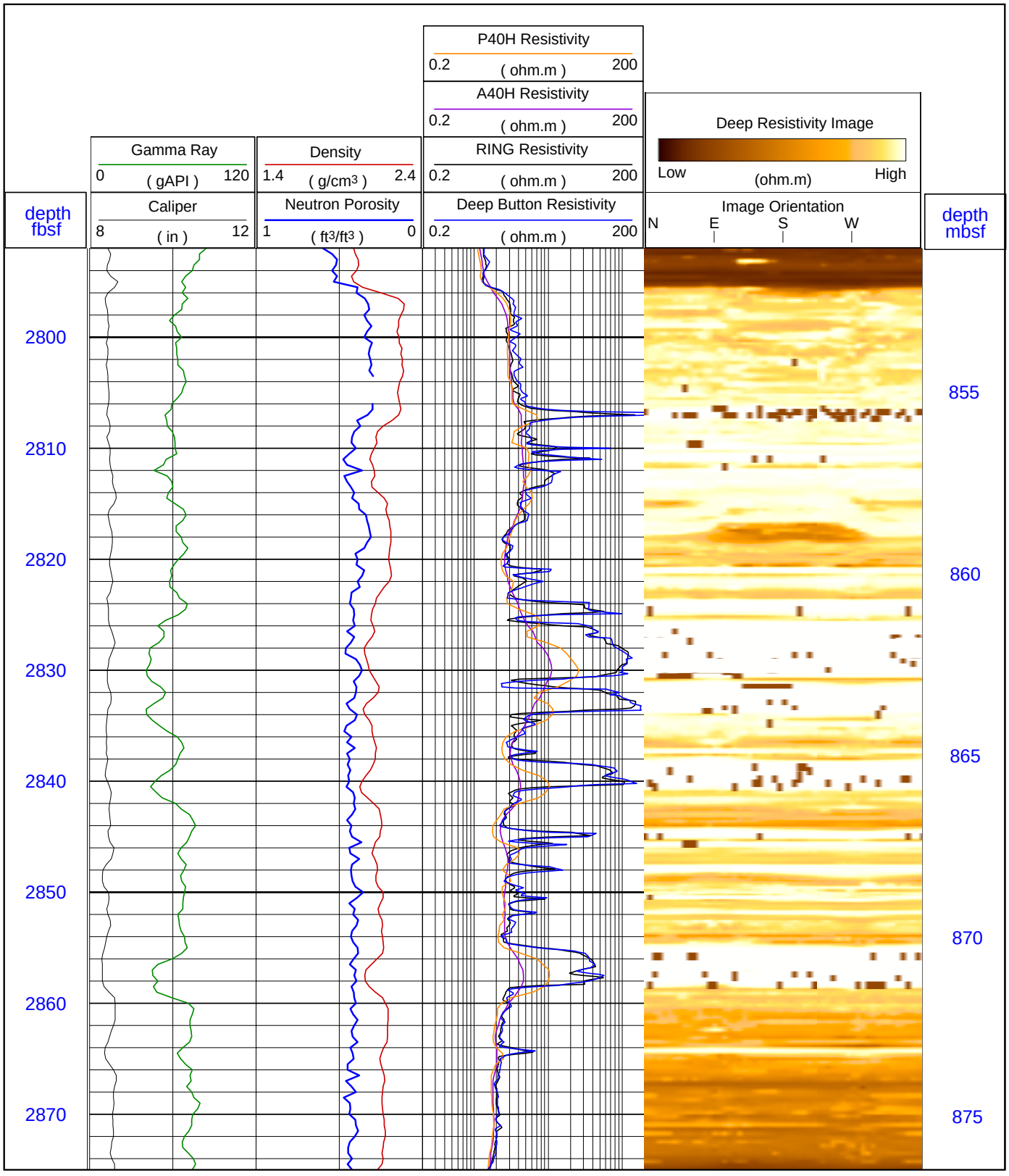

Figure F11: *Logs and LWD resistivity image from 2792-2875 fbsf in Hole WR 313-G depicting the target sand layer. Ring = Ring resistivity (geoVISION); P40H = Phase-shift resistivity at 2 MHZ and a transmitter-receiver spacing of 40 inches (EcoScope); A40H = Attenuation resistivity measured at 2 MHz and a transmitter-receiver spacing of 40 inches. (EcoScope).*

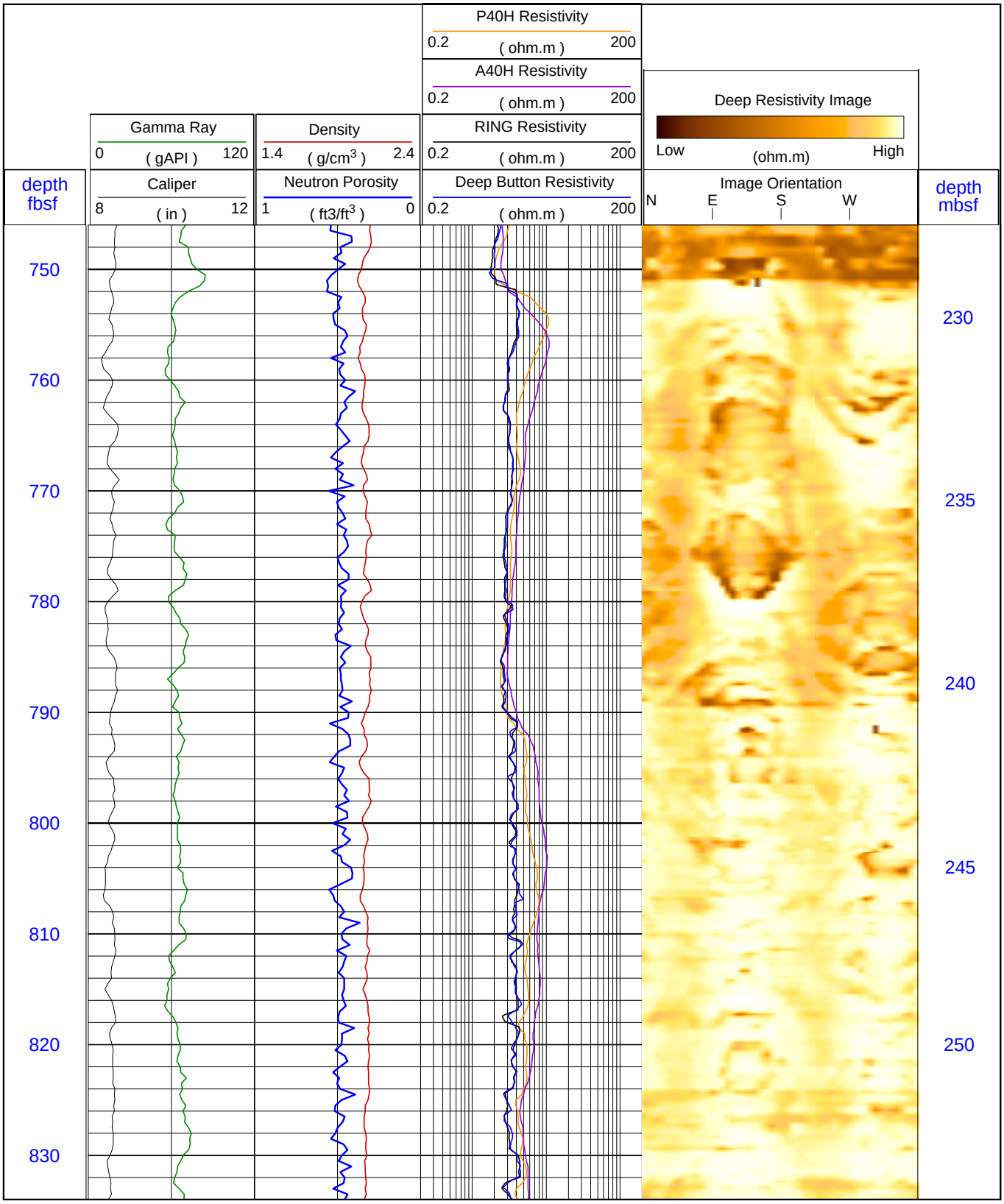

Figure F12: *Logs and LWD resitivity image from 746-834 fbsf in Hole WR 313-H depicting near vertical gas hydrate-filled fractures. Ring = Ring resistivity (geoVISION); P40H = Phase-shift resistivity at 2 MHZ and a transmitter-receiver spacing of 40 inches (EcoScope); A40H = Attenuation resistivity measured at 2 MHz and a transmitter-receiver spacing of 40 inches. (EcoScope).*

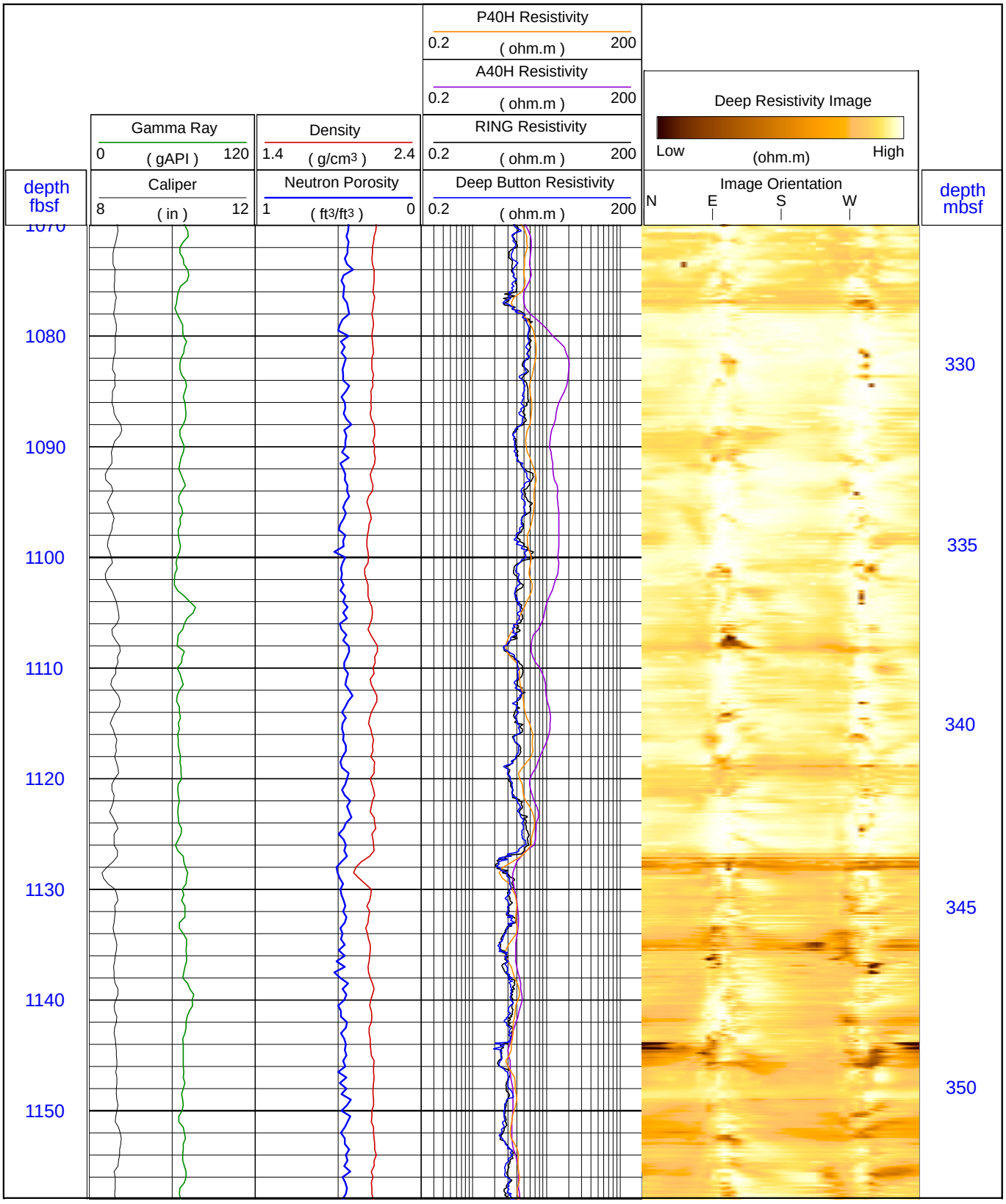

Figure F13: *Logs and LWD resistivity image from 1070-1158 fbsf in Hole WR 313-G depicting borehole breakouts through what are likely high-angle gas hydrate-filled fractures. Ring = Ring resistivity (geoVISION); P40H = Phase-shift resistivity at 2 MHZ and a transmitter-receiver spacing of 40 inches (EcoScope); A40H = Attenuation resistivity measured at 2 MHz and a transmitter-receiver spacing of 40 inches. (EcoScope).*

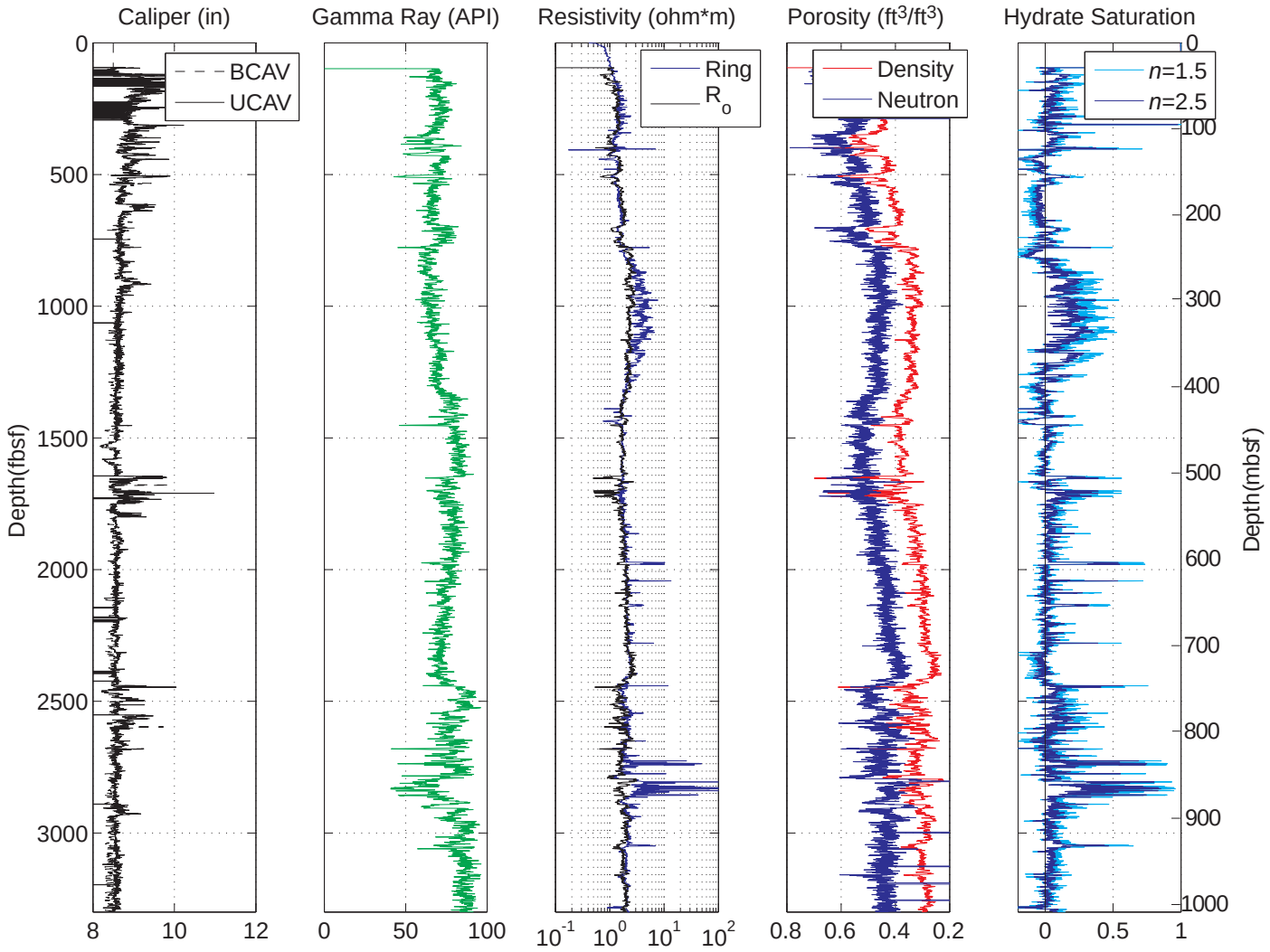

Figure F14: *Hydrate saturations from Archie's equation and LWD porosity and resistivity logs in Hole WR 313-G. BCAV = best density caliper; UCAV= ultrasonic density caliper; Ring = Ring resistivity (geoVISION); R_0 = Computed formation resistivity for 100% water saturation.*

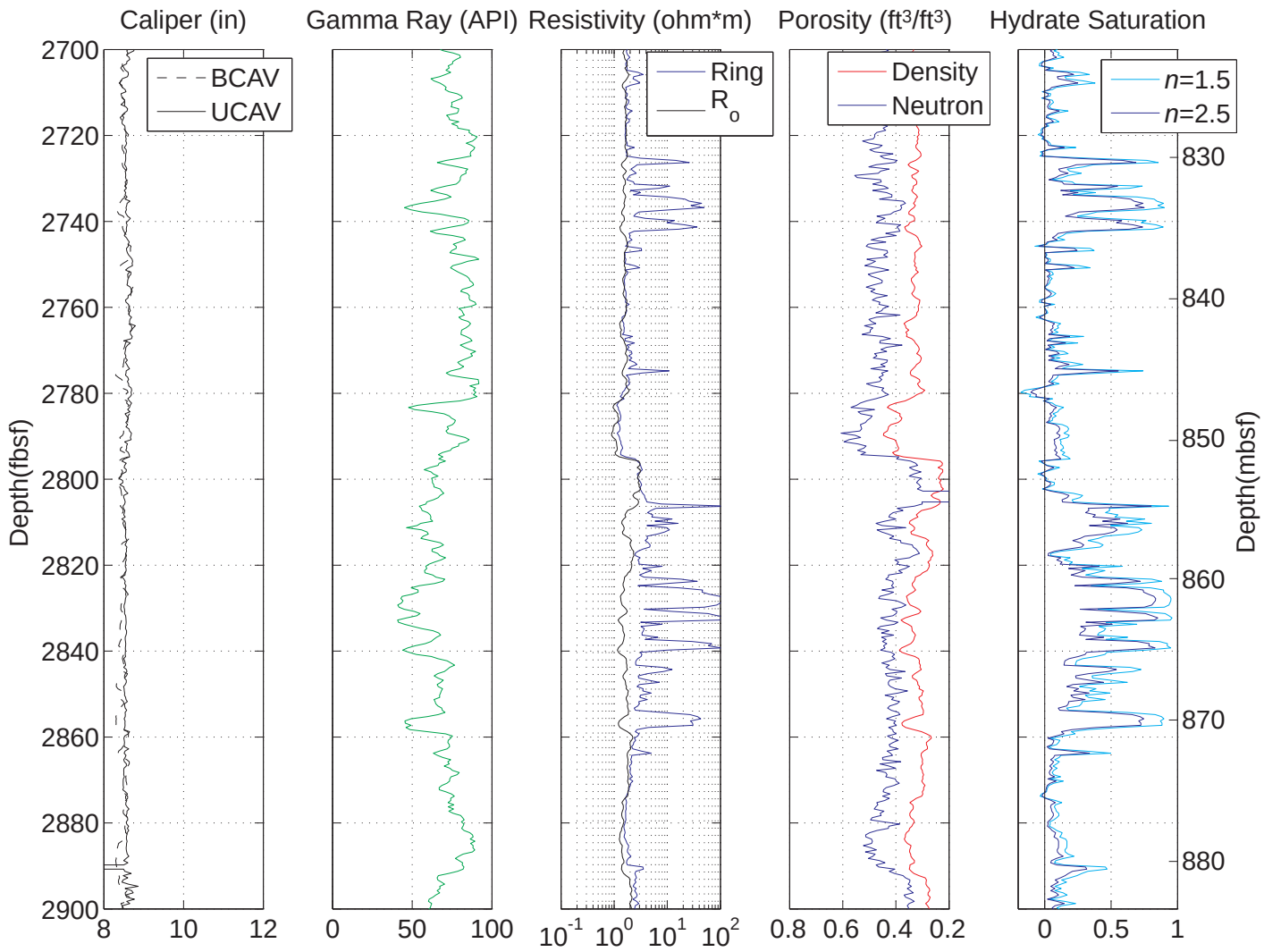

Figure F15: *Hydrate saturations from Archie's equation and LWD porosity and resistivity logs in Hole WR 313-G for the target sand layers from 2700-2900 fbsf. BCAV = best density caliper; UCAV= ultrasonic density caliper; Ring = Ring resistivity (geoVISION); R_0 = Computed formation resistivity for 100% water saturation.*

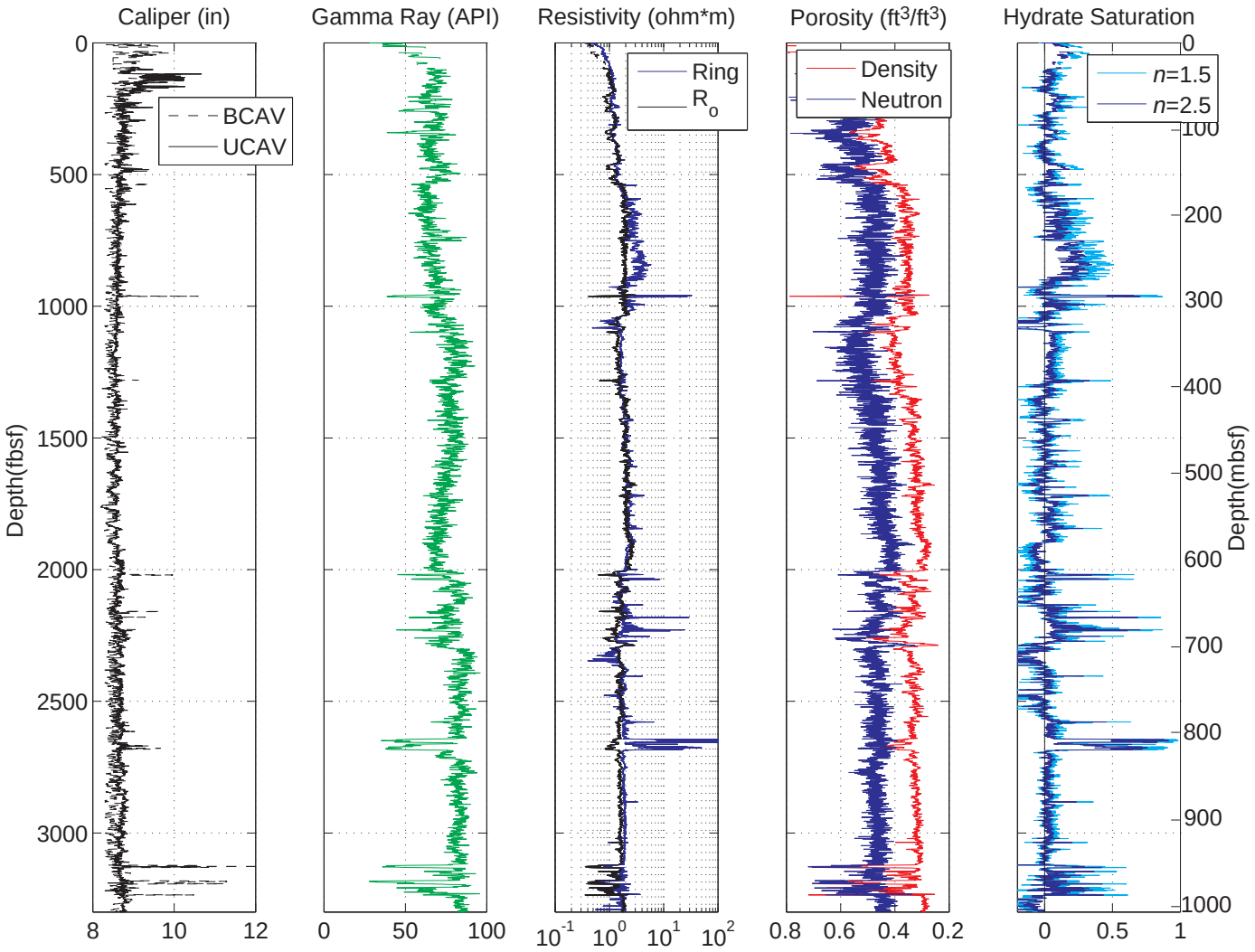

Figure F16: *Hydrate saturations from Archie's equation and LWD porosity and resistivity logs in Hole WR 313-H. BCAV = best density caliper; UCAV= ultrasonic density caliper; Ring = Ring resistivity (geoVISION); R_0 = Computed formation resistivity for 100% water saturation.*

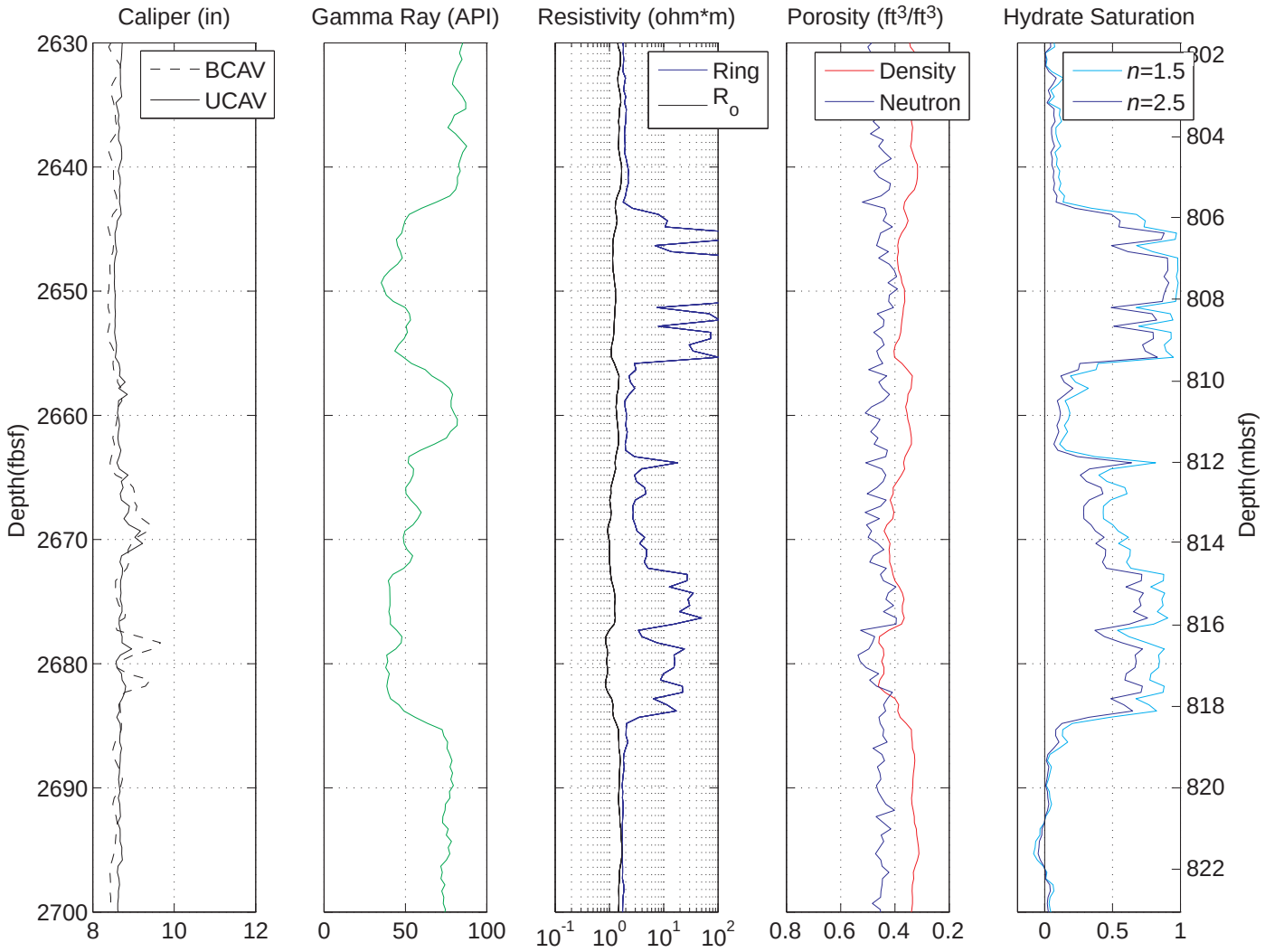

Figure F17: *Hydrate saturations from Archie's equation and LWD porosity and resistivity logs in Hole WR 313-H for the target sand layers from 2630-2700 fbsf. BCAV = best density caliper; UCAV= ultrasonic density caliper; Ring = Ring resistivity (geoVISION); R_0 = Computed formation resistivity for 100% water saturation.*

References

Collett, T.S., Boswell, R., Mrozewski, S., Guerin, G., Cook, A., Frye, M., Shedd, W., and McConnell, D., 2009. Gulf of Mexico Gas Hydrate Joint Industry Project Leg II — Operational Summary: Proceedings of the Drilling and Scientific Results of the 2009 Gulf of Mexico Gas Hydrate Joint Industry Project Leg II. http://www.netl.doe.gov/technologies/oil-gas/publications/Hydrates/2009Reports/OpSum.pdf

Hutchinson, D., Boswell, R., Collett, T.S., Dai, J., Dugan, B., Frye, M., Jones, E., McConnell, D., Rose, K., Ruppel, C., Shedd, W., Shelander, D., Wood, W., 2009. Gulf of Mexico Gas Hydrate Joint Industry Project Leg II — Walker Ridge 313 Site Selection: Proceedings of the Drilling and Scientific Results of the 2009 Gulf of Mexico Gas Hydrate Joint Industry Project Leg II http://www.netl.doe.gov/technologies/oil-gas/publications/Hydrates/2009Reports/WR 313SiteSelect.pdf

Lee, M. W. and T. S. Collett, 2009. Gas hydrate saturations estimated from fractured reservoir at Site NGHP-01-10, Krishna-Godavari Basin, India, J. Geophys. Res.114.10.1029/2008jb006237

McConnell, D., Boswell, R., Collett, T.S., Frye, M., Shedd, W., Guerin, G., Cook, A., Mrozewski, S., Dufrene, R., and Godfriaux, P., 2009. Gulf of Mexico Gas Hydrate Joint Industry Project Leg II — Walker Ridge 313 Site Summary: Proceedings of the Drilling and Scientific Results of the 2009 Gulf of Mexico Gas Hydrate Joint Industry Project Leg II. http://www.netl.doe.gov/technologies/oil-gas/publications/Hydrates/2009Reports/WR 313SiteSum.pdf

Mrozewski, S., Guerin, G., Cook, A., Collett, T.S., Boswell, R., 2009. Gulf of Mexico Gas Hydrate Joint Industry Project Leg II — LWD Methods: Proceedings of the Drilling and Scientific Results of the 2009 Gulf of Mexico Gas Hydrate Joint Industry Project Leg II. http://www.netl.doe.gov/technologies/oil-gas/publications/Hydrates/2009Reports/LWDMethods.pdf

Tréhu, A. M., *et al*., 2003. Drilling Gas Hydrates on Hydrate Ridge, Cascadia Continental Margin, College Station, TX (Ocean Drilling Program).